A high-resolution core-level photoemission study of the Au/4H-SiC(0001)-($\sqrt{3} \times \sqrt{3}$) interface

2007 J. Phys.: Condens. Matter 19 266006

(http://iopscience.iop.org/0953-8984/19/26/266006)

IOP PUBLISHING JOURNAL OF PHYSICS: CONDENSED MATTER

J. Phys.: Condens. Matter **19** (2007) 266006 (8pp) doi:10.1088/0953-8984/19/26/266006

A high-resolution core-level photoemission study of the Au/4H-SiC(0001)-($\sqrt{3} \times \sqrt{3}$) interface

D Stoltz[1], S E Stoltz[2] and L S O Johansson[3]

[1] Materialfysik, MAP, KTH-Electrum, SE-16440 Kista, Sweden
[2] MAX-Lab, Lund University, SE-22100 Lund, Sweden
[3] Department of Physics, Karlstad University, SE-65188 Karlstad, Sweden

E-mail: dunjap@kth.se

Received 25 April 2007, in final form 18 May 2007
Published 14 June 2007
Online at stacks.iop.org/JPhysCM/19/266006

Abstract

We present a systematic study of different reconstructions obtained after deposition of Au on the ($\sqrt{3} \times \sqrt{3}$)-R30°-4H-SiC(0001) surface. For 1–2 monolayers (ML) Au and annealing temperature $T_{\text{anneal}} \sim 675\,^{\circ}\text{C}$, a 3×3 reconstruction was observed. For 4 ML Au and $T_{\text{anneal}} \sim 650\,^{\circ}\text{C}$, a ($2\sqrt{3} \times 2\sqrt{3}$)-R30° reconstruction appeared, while 5 ML Au annealed at 700 °C reconstructed to give a ($6\sqrt{3} \times 6\sqrt{3}$)-R30° pattern. From the Si 2p and Au 4f core-level components, we propose interface models, depending on the amount of Au on the surface and the annealing temperature. For 1–4 ML Au annealed at 650–675 °C, gold diffuses under the topmost Si into the SiC and forms a silicide. An additional Si component in our Si 2p spectra is related to the interface between the silicide and SiC. For 5 ML Au annealed at 700 °C, silicide is also formed at the surface, covering unreacted Au on top of the SiC substrate. The interface Si component is also observed in the Si 2p spectra of this surface. The key role in Au/$\sqrt{3}$-4H-SiC(0001) interface formation is played by diffusion and the silicon-richness of the surface.

1. Introduction

Au on Si has been one of the most interesting systems for both applications in electronic devices and fundamental studies of interface formation and diffusion in the past decades. It has been clear since the earliest studies that strong interdiffusion of both Au in Si and Si in Au drives a complex interface formation in Au/Si [1, 2]. In the case of Si(111) as a substrate, the result is silicide (Au_3Si) at the surface covering some unreacted gold on top of the Si substrate [3, 4]. In contrast, Au on a Si(100) surface gives a silicide embedded between the Si at the surface and the bulk Si sample [5].

The interest in the Au/SiC interface has been growing during the past decade, as SiC started replacing Si in high-temperature, high-speed, high-power and high-voltage sensor

and electronic devices [6]. Investigations of Au/4H-SiC(000$\bar{1}$) reveal silicide at the surface, covering unreacted gold on top of the SiC sample [7], which is very similar to the interface formation between gold and Si(111). On the surface of 4H-SiC(0001), more silicon-rich (3×3, ($\sqrt{3}\times\sqrt{3}$)-R30°) or more carbon-rich reconstructions (($6\sqrt{3}\times6\sqrt{3}$)-R30°) can be obtained after different surface preparations [8], and they can serve as substrates for gold deposition. Studies of gold deposition on the 3×3 surface show the appearance of several different reconstructions depending on the post-anneal temperature [9]. For the ($2\sqrt{3}\times2\sqrt{3}$)-R30° reconstruction, an interface consisting of Si at the surface followed by silicide layer followed by SiC has been proposed [9]. This is clearly different than the observed Au/4H-SiC(000$\bar{1}$) interface, but essentially the same as the one for Au/Si(100). A similar interface has been seen in 3×3-reconstructed Au on ($\sqrt{3}\times\sqrt{3}$)-R30°-4H-SiC [9].

In this paper we present a systematic study of different reconstructions obtained after deposition of Au on the ($\sqrt{3}\times\sqrt{3}$)-R30° SiC surface. We correlate coverages and post-annealing temperatures with different reconstructions. Using synchrotron radiation based photoelectron spectroscopy we analyse the emission angle dependence of the intensities of different core-level components, to obtain information about their surface character or bulk character. Finally, we propose models for interfaces, depending on the amount of Au on the surface and the annealing temperature.

2. Experimental details

The experiments were performed at beamline 33 at the MAX-lab synchrotron in Lund. Beamline 33 is bending magnet based, and it allows for photon energies in the range between 15 and 200 eV. The end station is an angle-resolving VG analyser (ARUPS 10), which was used in this study with angular resolution of ±2° and energy resolution of $\leqslant$100 meV. The detector is rotatable in two angular degrees of freedom: in the horizontal and in the vertical plane. The sample manipulator is also rotatable around two axes: the polar axis and the azimuthal axis. The polar angle was set to give an incidence angle of the light of 45°. The azimuthal orientation of the sample was monitored by low-energy electron diffraction (LEED). The base pressure of the analysis chamber was 4×10^{-11} mbar, while that of the preparation chamber was in the lowest 10^{-10} mbar region.

The 4H-SiC(0001) wafer with 8° miscut in the [11$\bar{2}$0] direction was purchased from Cree. It is a high-quality (low micropipe) n-type wafer polished on both sides. Precleaning was performed in methanol and by HF (5%) etching before the introduction in the UHV chamber. *In situ* preparation started with outgassing at $T < 600\,^{\circ}$C. A well-ordered 3×3 surface was obtained after 30 min anneal of the sample at 800 °C in ∼2 ML 5 min^{-1} Si flux [8, 10, 11]. The ($\sqrt{3}\times\sqrt{3}$)-R30° reconstruction (short $\sqrt{3}$) was obtained by annealing the sample for an additional 30 min at 1000 °C with no Si flux [8, 10, 11]. For temperature reading a pyrometer was used, with the emissivity 0.85 [11]. The temperature gradient over the sample was ∼50 °C, which might have led to the onset of ($6\sqrt{3}\times6\sqrt{3}$)-R30° reconstruction at the highest-temperature end of the sample.

Gold was deposited on the ($\sqrt{3}\times\sqrt{3}$)-R30° surface from a W filament carrying a Au piece at ∼0.5 ML min^{-1}. Deposited films were post-annealed at 650–700 °C (due to the already-mentioned temperature gradient) for 5 min. The same emissivity value has been used for the pyrometer readings as in the case of the clean surface. The appearance and the quality of the reconstructions was checked by LEED. The sample was then cooled with liquid nitrogen for the photoelectron spectroscopy measurements. The Au coverages were estimated from the core-level intensities and quartz microbalance measurements.

Fermi level correction was performed according to the Fermi edge measurements on a tantalum foil under the same experimental conditions as in the Au/SiC experiment. The

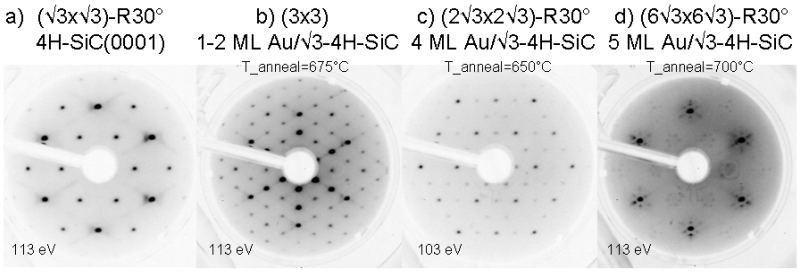

Figure 1. LEED patterns of (a) $(\sqrt{3} \times \sqrt{3})$-R30°-4H-SiC(0001) (short $\sqrt{3}$-4H-SiC); (b) (3×3) 1–2 ML Au/$\sqrt{3}$-4H-SiC; (c) $(2\sqrt{3} \times 2\sqrt{3})$-R30° 4 ML Au/$\sqrt{3}$-4H-SiC; (d) $(6\sqrt{3} \times 6\sqrt{3})$-R30° 5 ML Au/$\sqrt{3}$-4H-SiC. The post-anneal temperatures applied on the sample after gold deposition are marked on top. The LEED beam energy is marked in the lower-left corner.

Table 1. Acronyms used throughout this paper for different surfaces.

Surface	Reconstruction	T_{anneal} (°C)	Acronym
4H-SiC(0001)	$(\sqrt{3} \times \sqrt{3})$-R30°	—	$\sqrt{3}$-4H-SiC
1 ML Au/$\sqrt{3}$-4H-SiC	3×3	675	1 ML Au-3×3
2 ML Au/$\sqrt{3}$-4H-SiC	3×3	675	2 ML Au-3×3
4 ML Au/$\sqrt{3}$-4H-SiC	$(2\sqrt{3} \times 2\sqrt{3})$-R30°	650	4 ML Au-$2\sqrt{3}$
5 ML Au/$\sqrt{3}$-4H-SiC	$(6\sqrt{3} \times 6\sqrt{3})$-R30°	700	5 ML Au-$6\sqrt{3}$

intensities were calibrated with respect to the synchrotron current and the number of sweeps. The FITXPS2 software [12] was used for core-level fits.

3. Results

In figure 1(a) the LEED pattern of the substrate SiC surface, which was used for all gold depositions, is shown. It depicts the $(\sqrt{3} \times \sqrt{3})$-R30° reconstruction on the 4H-SiC(0001) ($\sqrt{3}$-4H-SiC). In figures 1(b)–(d) three different surface reconstructions are shown, which can be obtained by depositing and post-annealing gold on the $\sqrt{3}$-4H-SiC. In figure 1(b) a 3×3 reconstruction characteristic for small Au coverages (1–2 ML) and post-annealing temperatures of 675 °C (see figure 2) is presented. The one shown in the image was obtained for 2 ML Au. This reconstruction has been reported in similar conditions in [9]. In figure 1(c) a $(2\sqrt{3} \times 2\sqrt{3})$-R30° (short $2\sqrt{3}$) reconstruction is shown. It appears for coverages of 4–5 ML and post-anneal temperatures of 650 °C (see figure 2). The one shown in the image was obtained for 4 ML Au. On the other hand, the $(6\sqrt{3} \times 6\sqrt{3})$-R30° reconstruction (short $6\sqrt{3}$) is characteristic for 2–5 ML of Au on $\sqrt{3}$-4H-SiC post-annealed at 700 °C (see figure 2). The pattern shown in the image was obtained for 5 ML Au. A certain role for appearance of this reconstruction is played by the slightly higher annealing temperature of the 4H-SiC(0001) at one part of the sample, which may induce onset of $(6\sqrt{3} \times 6\sqrt{3})$-R30° reconstruction already on the pure substrate. We have not, however, observed the $6\sqrt{3}$ LEED pattern prior to gold deposition. Between these three reconstructions badly defined LEED patterns have been observed in figure 2 (shaded area). These will not be considered in further analysis. Acronyms which will be used for different coverages, instead of the full names describing the substrate, adsorbate and the reconstruction, are summarized in table 1.

The LEED patterns in figures 1(a)–(c) correspond exactly to the given reconstruction. In contrast, an identical $6\sqrt{3}$ LEED pattern as shown in figure 1(d) has been shown to correspond

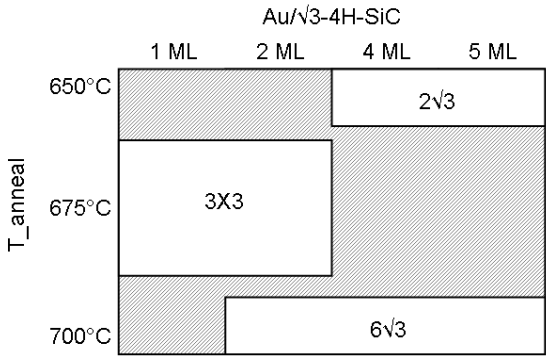

Figure 2. Schematic representation of gold coverage and anneal temperature dependent reconstructions on Au/$\sqrt{3}$-4H-SiC.

to a mixture of reconstructions on pure 6H-SiC(0001) [13–16]. Scanning tunnelling microscopy (STM) studies [13] show the presence of 5×5 and 6×6 patterns superimposed on to $(2.1\sqrt{3} \times 2.1\sqrt{3})$-R30°, with or without the $\sqrt{3}$ structure. Comparison with our LEED pattern reveals that $\sqrt{3}$ spots are not present in our case.

In figure 3, Si 2p core levels at normal emission (NE) and 45° off normal for 1, 2 ML Au-3×3 and 4 ML Au-$2\sqrt{3}$ are presented. The spectra correspond to the LEED patterns shown in figures 1(b) and (c). All spectra can be decomposed into three spin–orbit split doublets[4]. The doublet with the highest binding energy (dashed grey line) corresponds to SiC. At low coverages it is very similar to the Si 2p core level of the $\sqrt{3}$-4H-SiC surface (not shown), but it experiences a chemical shift of -0.7 eV upon Au exposure. Its intensity decreases with Au coverage, as expected.

The second doublet (bold grey line) is rather broad for all investigated coverages (total width of ∼0.5 eV) and exhibits a -0.8 eV shift with respect to the SiC peak in Au/$\sqrt{3}$-4H-SiC. This is the same as reported for silicide on Au/4H-SiC(000$\bar{1}$) [7] and for silicide on Au/4H-SiC(0001)-(3×3) [9]. We also assign this doublet to the silicide.

The third doublet (grey line) is sharper than the previous ones (total width of ∼0.3 eV) and has a binding energy at -1.1 eV from the SiC peak. For the lowest coverages it shows angular behaviour of a surface component, i.e. it increases in intensity at higher emission angles. At higher coverages, it shows angular-dependent intensity typical for an interface component. Due to its low width we attribute it to the Si at the surface or at the interface between Au–Si and SiC.

In figure 4, Au 4f core levels at normal emission for 1, 2 ML Au-3×3 and 4 ML Au-$2\sqrt{3}$ are presented. Only one spin–orbit split doublet is resolved in all Au 4f spectra. All spectra are thus fitted consistently with similar parameters for this doublet[5]. The binding energies are shifted by ∼0.54 eV towards the higher binding energies compared to reference values for pure gold (84/87.7 eV). The doublets are relatively broad (total width ∼0.9 eV), but the inclusion of another doublet is not supported by the spectral shape. This suggests that there is only one chemical species of Au, which according to the silicide component in the Si 2p spectra and according to the shift of the measured Au spectrum with respect to the bulk Au binding energies can only be attributed to the silicide.

[4] Si 2p spin–orbit split doublets were fitted with following parameters: 0.61 eV spin–orbit splitting, 0.5 branching ratio, 0.06–0.08 eV Lorentzian width and variable Gaussian width, 0.04–0.17 asymmetry parameter.

[5] Au 4f spin–orbit split doublets were fitted with following parameters: 3.67 eV spin–orbit splitting and 0.07–0.25 asymmetry parameter.

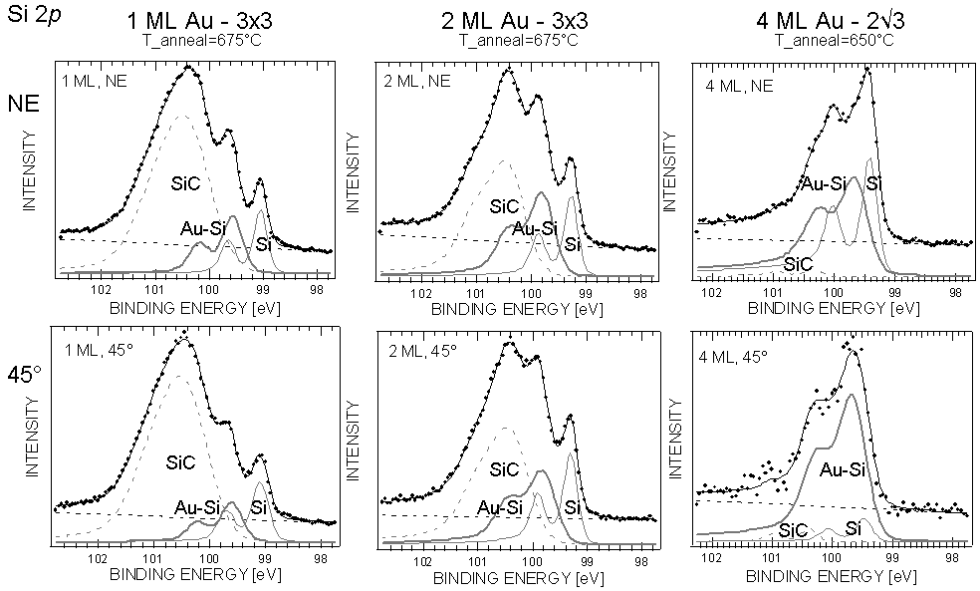

Figure 3. Si 2p core-level measurement (dots) and fit (black line) consisting of three spin–orbit split doublets (grey) and a linear background (dashed black line) at normal emission (NE) and 45° off normal for 1, 2 ML Au-3 × 3 (annealed at 675 °C) and 4 ML Au-2$\sqrt{3}$ (annealed at 650 °C). All spectra were measured with photon energy of 130 eV.

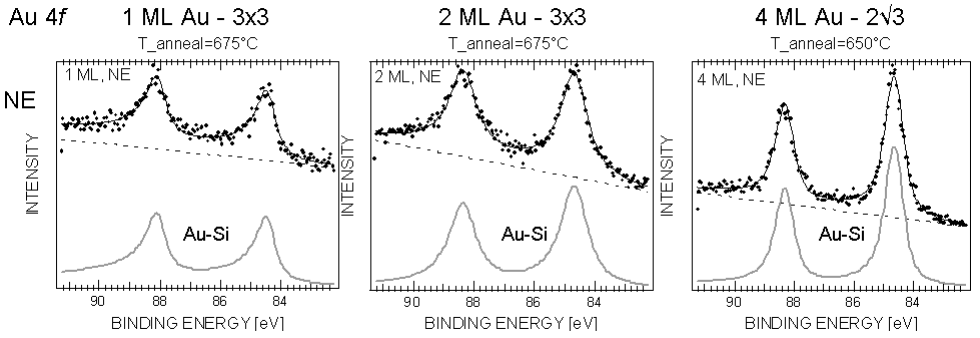

Figure 4. Au 4f core level measurement (dots) and fit (black line) consisting of one spin–orbit split doublet (grey) and a linear background (dashed black line) at normal emission (NE) for 1, 2 ML Au-3 × 3 (annealed at 675 °C) and 4 ML Au-2$\sqrt{3}$ (annealed at 650 °C). All spectra were measured with photon energy of 130 eV.

In figure 5, both Si 2p and Au 4f core levels at normal emission and 45° off normal for 5 ML of Au/$\sqrt{3}$-4H-SiC annealed at 700 °C are presented. This surface shows the 6$\sqrt{3}$ reconstruction from figure 1(d). As mentioned earlier, this reconstruction may be triggered by the slightly higher annealing of the clean SiC at that part of the sample, and thus the induced onset of the 6$\sqrt{3}$-SiC reconstruction. This was not seen by LEED, but some similarities between 5 ML Au-6$\sqrt{3}$ and 6$\sqrt{3}$-SiC exist in core levels. The Si 2p core level in figure 5 at NE covers similar binding energies as the one of the 6$\sqrt{3}$-SiC in figure 3(a) of [17].

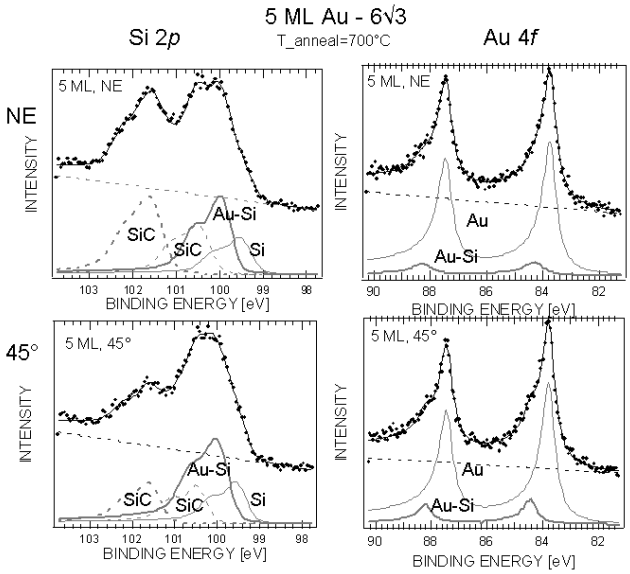

Figure 5. Si 2p and Au 4f core-level measurement (dots) and fit (black line) consisting of spin–orbit split doublets (grey) and a linear background (dashed black line) at normal emission (NE) and 45° off normal for 5 ML Au-6$\sqrt{3}$ annealed at 700 °C. All spectra were measured with photon energy of 130 eV.

However, the electronic structure of the 6$\sqrt{3}$ reconstruction on pure or gold-covered SiC is very different [18].

Our spectrum can be decomposed in four spin–orbit split doublets. Two of them (dashed grey lines) show bulk character. While one of them (dashed grey line) is at the same binding energy as the SiC component seen at 1–4 ML of Au, the second bulk-like peak (bold dashed grey line) appears at ∼1 eV higher binding energy than the SiC peak. This peak is similar to the one observed in [17] for 6$\sqrt{3}$-SiC, with a shift of 0.6 eV towards higher binding energies. Therefore, we also attribute it to the onset of 6$\sqrt{3}$ reconstruction (slightly higher annealing temperature) on the clean SiC [17].

The most pronounced doublet (bold grey line) is a surface component (see off normal emission) and is attributed to the silicide. At its lower binding energy side a surface peak due to interface Si is seen (grey line). Their binding energy shifts are similar to the ones on the previously discussed surfaces (−0.5 and −0.9 eV). The width of the silicide peak is still ∼0.6 eV, while the width of the Si peak is now ∼0.6 eV. This suggest less well-defined coordination of interface Si, contrary to the sharp Si peak at 1–2 ML Au originating from the well-ordered surface atoms.

In the Au 4f spectra in figure 5, two different doublets can be clearly resolved. The higher binding energy one (bold grey line) is at approximately the same binding energy as the doublet in 1–4 ML Au, and it has a similar width of ∼0.85 eV. It has been assigned to the silicide and at 5 ML it has a surface character. On the lower binding energy side a much more intense doublet is observed (grey line). Its binding energy is 83.8/87.4 eV, very close to the reference Au values (84/87.7 eV) and its width is ∼0.68 eV. This doublet is assigned to a thick layer of unreacted gold below the surface. The shift between the two doublets is ∼0.65 eV, similar to that in [3, 7, 9].

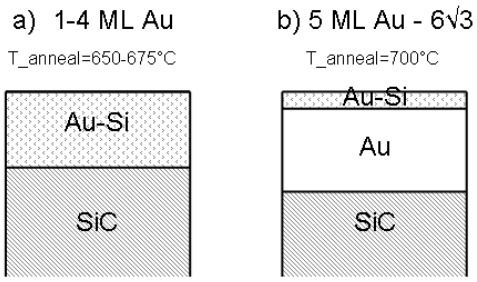

Figure 6. Schematic representation (not to scale!) of interface formation for (a) 1–4 ML Au annealed at $T_{\text{anneal}} = 650$–$675\,^{\circ}\text{C}$ and (b) 5 ML Au-$6\sqrt{3}$ annealed at $T_{\text{anneal}} = 700\,^{\circ}\text{C}$.

4. Discussion

In figure 6, models for the Au/$\sqrt{3}$-4H-SiC interface have been proposed based on the core-level results presented in previous figures. In these models, only SiC, Au–Si and Au have been taken into account, for simplicity. All the interface or surface Si components have been left out. For 1–4 ML and annealing at 650–675 °C (figure 6(a)), gold diffuses under the surface and forms a silicide layer. An additional component in the Si 2p spectra suggests that an interfacial Si layer develops between the surface silicide and buried SiC. In figure 6(b) the interface of 5 ML Au-$6\sqrt{3}$ annealed at 700 °C is shown. Silicide is at the surface, but underneath it is unreacted Au. Below them is SiC, which contributes with two bulk-like peaks to the Si 2p lineshape.

With increasing amount of gold, an increasingly large layer of silicide is formed at the surface at annealing temperatures of 650–675 °C. While the annealing temperature is crucial for the reconstruction at the surface, variations between 650 and 675 °C do not seem to play a role for interface formation. Both diffusion of gold and silicon is relevant for the silicide formation. As the surface that we measured was always liquid nitrogen cooled after preparation, we made sure that the diffusion was stopped and that we were looking at the non-changing system. For a bit higher annealing temperatures (700 °C), gold aggregation replaces silicide formation. Specific interface formation at 5 ML Au-$6\sqrt{3}$ is also related to the $6\sqrt{3}$ reconstruction. At the clean SiC surface, this reconstruction is carbon-rich. Higher annealing temperatures lead to silicon depletion at the surface and this depletion can be responsible for smaller amount of Si available for silicide formation.

Finally, photoelectron spectroscopy from a well-ordered surface is not free of photoelectron diffraction effects. These could influence the core-level intensity changes at 45° emission angle, which were used in this study. It is therefore important to notice that identification of the surface components in our spectra has been done based on the core-level shifts, peak widths and comparisons with the literature. The core-level spectra recorded at 45° emission angle agree very well with these findings. However, one conclusion could be affected by photoelectron diffraction. The placement of silicide on the surface within the interface model for 5 ML Au-$6\sqrt{3}$ annealed at 700 °C (figure 6(b)) was based on the observation that the silicide component in the Au 4f core level becomes stronger at 45°. If this was influenced by the photoelectron diffraction, the order of Au and Au–Si would simply change in figure 6(b): Au would be lying on top, while silicide would be at the interface between Au and SiC. In the absence of photoelectron diffraction data, we leave figure 6(b) as it is, because it is in good agreement with already reported interfaces of Au/Si(111) [3, 4] or Au/4H-SiC(000$\bar{1}$) [7].

5. Conclusions

A systematic study of different reconstructions obtained after deposition of Au on the ($\sqrt{3} \times \sqrt{3}$)-R30°-4H-SiC(0001) is presented. For 1–2 ML Au and $T_{\text{anneal}} \sim 675\,^{\circ}\text{C}$ a 3×3-

reconstruction was observed. For 4 ML Au and $T_{\text{anneal}} \sim 650\,^{\circ}\text{C}$, a $(2\sqrt{3} \times 2\sqrt{3})$-R30° reconstruction appeared, while 5 ML Au annealed at 700 °C reconstructed to give a $(6\sqrt{3} \times 6\sqrt{3})$-R30° pattern. From the Si 2p and Au 4f core-level components, we propose interface models, depending on the amount of Au on the surface and annealing temperature. For 1–4 ML Au annealed at 650–675 °C, gold diffuses under the topmost Si into the SiC and forms a silicide. An additional Si component in our Si 2p spectra is related to the interface between the silicide and SiC. For 5 ML Au annealed at 700 °C, silicide is also formed at the surface, covering unreacted Au on top of the SiC substrate. An interface Si component is also observed in the Si 2p spectra of this surface. Diffusion and silicon-richness of the surface are determining factors behind this interface formation.

Acknowledgments

We would like to thank T Balasubramanian (MAX-lab) for help at the beamline and K O Magnusson (Karlstad University) and M Göthelid (KTH Kista) for useful discussions. The Göran Gustafsson Foundation is kindly acknowledged for financial support.

References

[1] Braicovich I, Garner C M, Skeath P R, Su C Y, Chye P W, Lindau I and Spicer W E 1979 *Phys. Rev.* B **20** 5131
[2] Sarkar D K, Bera S, Dhara S, Nair K G M, Narasimhan S V and Chowdhury S 1997 *Appl. Surf. Sci.* **120** 159
[3] Molodtsov S L, Laubschat C, Kaindl G, Shikin A M and Adamchuk V K 1991 *Phys. Rev.* B **44** 8850
[4] Yeh J-J, Hwang J, Bertness K, Friedman D J, Cao R and Lindau I 1993 *Phys. Rev. Lett.* **70** 3768
[5] Haruyama Y, Kanda K and Matsui S 2004 *J. Electron Spectrosc. Relat. Phenom.* **137–140** 97
[6] O'Connor J R and Smiltens J (ed) 1960 *Silicon Carbide—A High Temperature Semiconductor* (Oxford: Pergamon)
[7] Virojanadara C and Johansson L I 2005 *Surf. Sci.* **585** 163
[8] Heinz K, Bernhardt J, Schardt J and Starke U 2004 *J. Phys.: Condens. Matter* **16** S1705
[9] Virojanadara C and Johansson L I 2006 *Surf. Sci.* **600** 436
[10] Starke U, Schardt J and Franke M 1997 *Appl. Phys.* A **65** 587
[11] Ostedorf R, Wulff K, Benesch C, Merz H and Zacharias H 2004 *Phys. Rev.* B **70** 205325
[12] Adams D L 2001 fitxps2 peak-fitting software www.sljus.lu.se/download.html version 2.12
[13] Owman F and Mårtensson P 1996 *Surf. Sci.* **369** 126
[14] Owman F and Mårtensson P 1995 *J. Vac. Sci. Technol.* B **14** 933
[15] Marumoto Y, Tsukamoto T, Hirai M, Kusaka M, Iwami M, Ozawa T, Nagamura T and Nakata T 1995 *Japan. J. Appl. Phys.* **34** 3351
[16] Li L and Tsong I S T 1996 *Surf. Sci.* **351** 141
[17] Johansson L I, Owman F and Mårtensson P 1996 *Surf. Sci.* **360** L483
[18] Stoltz D, Stoltz S E and Johansson L S O 2007 *Surf. Sci.* http://dx.doi.org/10.1016/j.susc.2007.04.078